

ORIGINAL ARTICLE

Shp2 promotes metastasis of prostate cancer by attenuating the PAR3/PAR6/aPKC polarity protein complex and enhancing epithelial-to-mesenchymal transition

K Zhang¹, H Zhao¹, Z Ji¹, C Zhang¹, P Zhou¹, L Wang¹, Q Chen¹, J Wang¹, P Zhang², Z Chen³, HH Zhu¹ and W-Q Gao¹

Epithelial-to-mesenchymal transition (EMT), marked by the dissolution of cell–cell junctions, loss of cell polarity and increased cell motility, is one of the essential steps for prostate cancer metastasis. However, the underlying mechanism has not been fully explored. We report in this study that Shp2 is upregulated in prostate cancers and is associated with a poor disease outcome, namely tumor metastasis and shortened patient survival. Overexpression of wild-type Shp2 or an oncogenic Shp2 mutant leads to increased prostate cancer cell proliferation, colony and sphere formation, and *in vivo* tumor formation. Opposite effects are seen in Shp2-knockdown cells. Moreover, Shp2 promotes *in vitro* migration and *in vivo* metastasis of prostatic tumor cells. Mechanistically, Shp2 interacts with PAR3 (partitioning-defective 3) via its Src homology-2 domain. Ectopic expression of Shp2 attenuates the phosphorylation of PAR3 and the formation of the PAR3/PAR6/atypical protein kinase C polarity protein complex, resulting in disrupted cell polarity, dysregulated cell–cell junctions and increased EMT. These findings provide a novel mechanism by which oncogenic signal-transduction molecules regulate cell polarity and induction of EMT.

Oncogene (2016) 35, 1271–1282; doi:10.1038/onc.2015.184; published online 8 June 2015

INTRODUCTION

Prostate cancer is the most frequently diagnosed cancer among males in the Western world, and its incidence steadily increases in developing countries including China.¹ Owing to the absence of an effective cure for advanced disease, especially that involving metastasis, prostate cancer remains the second leading cause of cancer-related death in the United States.² Understanding the molecular mechanisms governing prostate tumor progression and metastasis is critical for the development of new therapeutic methods.

Recently accumulated evidence suggests that epithelial-to-mesenchymal transition (EMT) is a necessary biological process for tumor metastasis. During EMT, epithelial cells lose basal–apical cell polarity and cell–cell junctions so as to acquire mesenchymal motile phenotypes.^{3–5} A group of evolutionarily conserved partitioning-defective (PAR) proteins orchestrate the generation of the apical and basolateral domains and contribute to the formation of tight junctions (TJs) between polarized epithelial cells.⁶ The restricted spatial localization of PAR proteins is essential for the maintenance of epithelial polarity.⁷ For example, the PAR3/PAR6/atypical protein kinase C (aPKC) protein complex localizes to the apical–lateral boundary region where TJ are formed, whereas PAR1 is usually concentrated in the lateral domain.^{7,8} Extensive research has shown that signaling among different PAR complex members and changes in their protein phosphorylation status are responsible for the asymmetric distribution of PAR proteins.⁹ However, it is not fully understood as to how extracellular stimuli and intracellular signaling pathways modulate the polarity protein

complex during EMT. Toward this end, Aranda *et al.*¹⁰ demonstrated that activated receptor tyrosine kinase ErbB2 interacts with PAR6/aPKC and uncouples the association between PAR3 and aPKC, resulting in disrupted apical polarity of breast epithelial cells. Wang *et al.*¹¹ showed that upon stimulation by multiple growth factors, PAR3 could be phosphorylated by Src kinases such as c-Src and c-Yes, which is required for its association with LIM kinase 2 and for the assembly of epithelial TJ.¹¹ *Helicobacter pylori* cytotoxin-associated gene A complexes with PAR1, inhibiting PAR3-mediated phosphorylation of PAR1 and releasing it from the basolateral membrane to cause the loss of gastric epithelial cell polarity.¹² Importantly, upon association with PAR1, cytotoxin-associated gene A is phosphorylated by Src kinases, followed by docking and activation of the Shp2 oncoprotein, resulting in elevated mitogenic and cell motility-promoting signals.

Shp2 is a tyrosine phosphatase with two amino-terminal Src homology-2 (SH2) domains, and it acts to amplify signals emanating from receptor tyrosine kinases or cytoplasmic tyrosine kinases.^{13,14} Dominantly activating mutations are detected in the *Ptpn11* gene encoding Shp2 in 50% of Noonan syndrome (NS) patients, who exhibit higher risk of hepatosplenomegaly and juvenile myelomonocytic leukemia.¹⁵ In addition, somatic gain-of-function mutations has been detected in several types of leukemia patients.¹⁶ However, recent studies have provided evidence that Shp2 may also function as a tumor suppressor in hepatocellular carcinoma.¹⁷ Still, in most other solid tumors examined, including breast cancer, lung cancer and neuroblastoma, Shp2 is generally considered to be an oncoprotein, promoting mitogenic and

¹State Key Laboratory of Oncogenes and Related Genes, Renji-MedX Clinical Stem Cell Research Center, Ren Ji Hospital, School of Biomedical Engineering, Shanghai Jiao Tong University, Shanghai, China; ²Key Laboratory of Systems Biology, Institute of Biochemistry and Cell Biology, Shanghai Institutes for Biological Sciences, Chinese Academy of Sciences, Shanghai, China and ³School of Life Science and Technology, Shanghai Tech University, Shanghai, China. Correspondence: Professor HH Zhu or Professor W-Q Gao, State Key Laboratory of Oncogenes and Related Genes, Renji-MedX Clinical Stem Cell Research Center, Ren Ji Hospital, School of Biomedical Engineering, Shanghai Jiao Tong University, 160 Pujian Road, Shanghai 200127, Shanghai, China.

E-mail: zhuhecrane@shsmu.edu.cn (HHZ) or gao.weiqiang@sjtu.edu.cn (W-QG)

Received 25 October 2014; revised 19 March 2015; accepted 24 April 2015; published online 8 June 2015

survival signaling.^{18–21} Furthermore, emerging evidence suggests that Shp2 facilitates migration, invasion and metastasis of breast cancer cells by modulating focal adhesion kinase (FAK) or Fyn downstream of growth factors or integrins.^{22–25} A recent study by Yang *et al.*²⁶ provides evidence that Gab1 binds to PAR1 and enhances PAR3 phosphorylation by PAR1, and serves as a negative regulator of epithelial TJ formation and cell polarity. Importantly, Gab1 is a scaffold protein that interacts with Shp2 upon multiple growth factor or cytokine stimulation.^{27,28} Therefore, whether Shp2 contributes to the dynamic regulation of the PAR protein complex in prostate epithelia and has a role in EMT and metastasis of prostatic tumors remains an important question.

We report in this study that Shp2 is upregulated in prostate cancers and is associated with advanced disease progression. Shp2 enhances prostate cancer cell proliferation, colony and sphere formation, and *in vivo* tumor formation. Moreover, Shp2 promotes *in vitro* migration and *in vivo* metastasis of prostatic tumor cells. Mechanistic studies show that Shp2 interacts with PAR3, attenuates the phosphorylation of PAR3 and the formation of the PAR3/PAR6/aPKC polarity protein complex, leading to the disruption of cell polarity and cell–cell junction, and thus the induction of EMT.

RESULTS

Shp2 is upregulated in human prostate cancers and positively correlates with advanced disease stage, tumor metastasis and shortened patient survival

To determine the clinical significance of Shp2 in prostate tumors, we first searched multiple microarray data in the *Oncomine* database. As shown in Figure 1a, Shp2 mRNA levels were significantly upregulated in human prostate cancer tissues. Elevated expression of Shp2 was associated with high-grade tumors (Gleason scores of 7 and 8 versus Gleason score of 6) (Figure 1a). In addition, the Shp2 expression level was significantly increased in lymph node metastases, and further upregulated in distal metastases compared with the primary site (Figures 1b and c). Notably, elevated Shp2 expression was strongly correlated with shortened prostate cancer patient survival (Figure 1d).

To confirm the Oncomine database analysis results, we compared the protein levels of Shp2 in clinically collected human prostate adenocarcinoma specimens and their paired adjacent normal tissues using immunoblotting and immunohistological staining. Among the 14 pairs of fresh samples examined by immunoblotting, 8 out of 14 patient samples showed elevated protein levels of Shp2 compared with their corresponding normal tissues (Figure 1e). In addition, upregulated Shp2 protein levels were found in 19 out of 29 pairs of paraffin-embedded prostate tumor samples examined by immunohistological staining (Figure 1f and Supplementary Table 1). A detailed description of the pathological diagnosis for the patient samples in this study is provided in Supplementary Table 1.

Shp2 promotes prostate cancer cell proliferation, colony and sphere formation *in vitro* and xenograft tumor formation *in vivo*

We first examined the Shp2 expression level in different prostate cancer cell lines. As shown in Supplementary Figure S1, the more aggressive prostate cancer cell lines DU145 and PC3 expressed more abundant Shp2 than LnCap cells. Therefore, to examine the biological function of Shp2 in prostate cancer, we constructed a short hairpin RNA (shRNA)-containing lentivirus to downregulate Shp2 in DU145 and PC3 cells. Efficient Shp2 knockdown was verified by immunoblotting and quantitative real-time (q-RT)-PCR (Figure 2a). We first investigated whether Shp2 influenced prostate cancer cell proliferation by propidium iodide staining for cell cycle analysis. As shown in Figure 2b, Shp2 knockdown decreased the percentage of cells in the S phase, thereby

reflecting a slowed cell proliferation rate of DU145 cells. In addition, Shp2 knockdown attenuated the colony-forming capability of DU145 cells, as the number of single-cell-derived colonies was markedly decreased (Figure 2c). Consistently, sphere-forming assay showed significantly reduced sphere number and smaller sphere size in Shp2-knockdown DU145 cells compared with the respective control cells (Figure 2d). Similar results were obtained from Shp2-knockdown PC3 cells (data not shown). To verify the positive role of Shp2 in prostate cancer growth *in vivo*, we performed xenograft tumor assays using DU145 cells stably transfected with either Shp2-shRNA or scramble lentiviruses. As shown in Figure 2e, Shp2 knockdown significantly inhibited prostate tumor growth in nude mice. In addition, attenuated xenograft tumor growth was observed in Shp2-knockdown PC3 cells (Figure 2f). To exclude the off-target effects of shRNA, we used an independent, second shRNA sequence against Shp2. As shown in Supplementary Figures S2A and C, knockdown of Shp2 by shShp2 no. 2 led to a similar suppression of prostate cancer cell proliferation and *in vivo* tumor growth.

Shp2 is a protein phosphatase composed of two SH2 domains, a phosphatase (PTPase) domain, a carboxy terminal tail and a proline-rich motif, with its enzymatic activity controlled by an autoinhibitory interaction between the amino-terminal SH2 domain and the phosphatase domain.²⁹ The presence of an activating mutation or elevated Shp2 protein level was reported in hematological malignancies and some types of solid tumor. To test whether Shp2 upregulation has an effect on prostate tumor growth and whether the effect is phosphatase dependent, we used a retroviral system to stably express flag-tagged wild-type (WT) Shp2 or dominant-active (DA) Shp2 in LnCaP cells (Figure 3a). Consistent with the Shp2-knockdown experimental data, expression of WT-Shp2 increased the portion of cells in the S phase, as determined by cell cycle analysis using propidium iodide staining. Ectopic expression of DA-Shp2 further promoted cell proliferation of LnCaP cells (Figure 3b). Expression of kinase-dead Shp2 (KD-Shp2, C459S mutant) slowed down the cell cycle progression of DU145 cells (Figure 3c). Moreover, overexpression of WT-Shp2 led to elevated colony- and sphere-forming capacity of LnCaP cells, and this effect was more profound in DA-Shp2 retroviral-infected cells (Figures 3d and e). To further test the impact of Shp2 on tumor growth *in vivo*, we inoculated nude mice with LnCaP or DU145 cells stably transfected with WT-Shp2, KD-Shp2 or control retrovirus and measured the tumor size weekly. As shown in Figures 3f and 3g, WT-Shp2 significantly increased the tumor growth *in vivo*, whereas KD-Shp2 expression led to a suppressed tumor growth *in vivo* (Figure 3h). In addition, we targeted Shp2 enzyme activity using a previously reported small-molecule Shp2 inhibitor II-B08.³⁰ As shown in Figure 3i, *in vivo* treatment of Shp2 inhibitor significantly repressed the xenograft prostate tumor growth. These data collectively suggested a stimulating role of Shp2 in prostate tumorigenesis, which is dependent on the phosphatase activity of Shp2.

Shp2 enhances prostate cancer cell mobility, migration and *in vivo* tumor metastasis

It was previously documented that by modulating FAK or Rho small G-protein (Rho) signaling, Shp2 contributes to cell scattering and migration of normal epithelial cells or breast cancer cells.^{22,23,31} Given that Shp2 level is upregulated in prostate cancer metastasis (Figures 1b and c), we asked the question of whether it has a positive role in the regulation of prostate cancer cell mobility and metastasis. Using a scratch assay, we found Shp2 knockdown significantly hindered the cell motility of DU145 cells (Figure 4a). In line with that, silencing of Shp2 resulted in a suppression of transwell migration of DU145 cells, whereas elevated migration was observed in WT or DA-Shp2 retrovirus-transfected

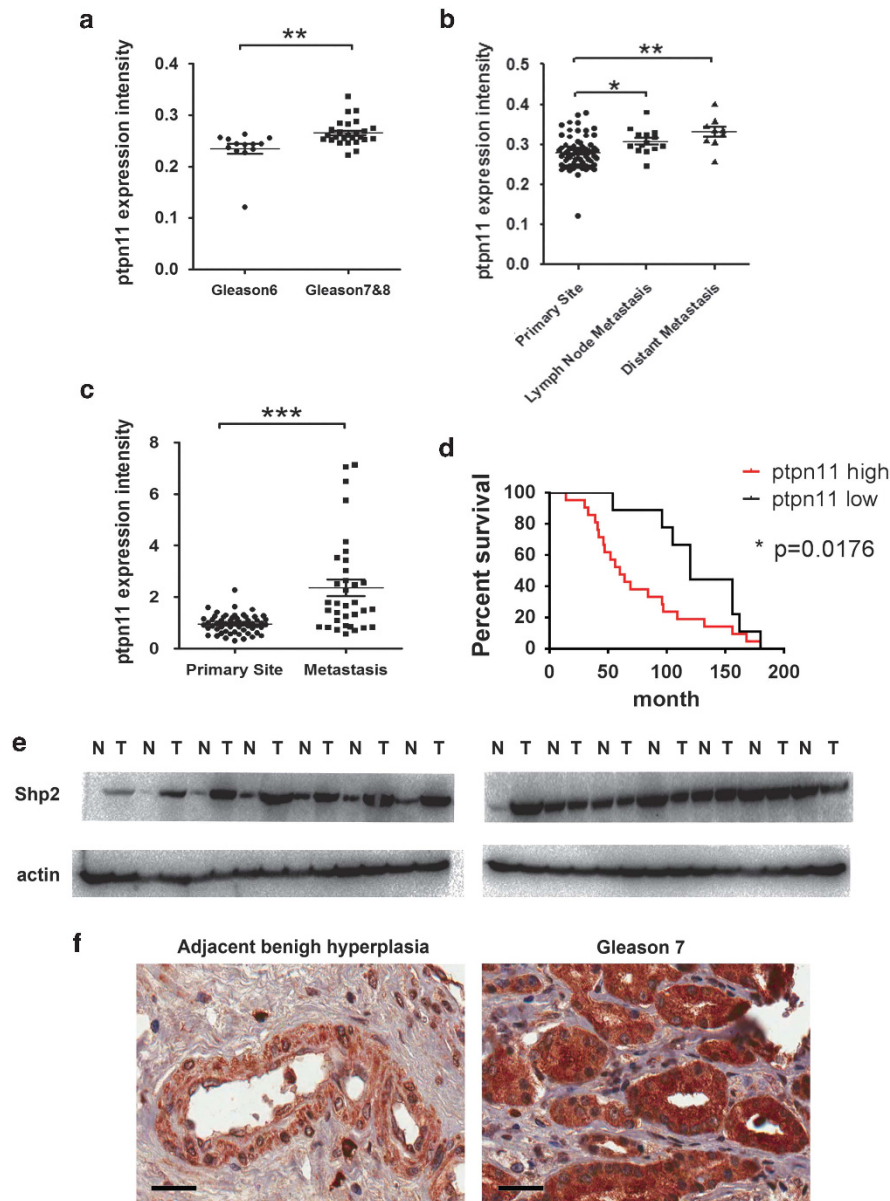


Figure 1. Shp2 is upregulated in prostate tumors and is associated with advanced disease stages and metastasis. **(a)** Analysis from the *Oncomine* online database shows that PTPN11 mRNA expression levels are significantly higher in prostate tumors with Gleason score 7 or 8 compared with those with Gleason score 6. Data were collected from the Liu cancer prostate cancer gene expression study⁴² (** $P < 0.01$, $n = 13, 26$). **(b)** mRNA levels of PTPN11 is upregulated in lymph node metastasis and further increased in distal metastasis compared with primary prostate tumors. Analysis was performed from the Yu cancer prostate cancer gene expression study⁴³ in the *Oncomine* database (** $P < 0.01$, * $P < 0.05$, $n = 63, 15, 9$). **(c)** Increased PTPN11 expression levels are significantly correlated with tumor metastasis. Analysis was performed from the Grasso cancer prostate cancer gene expression study⁴⁴ in the *Oncomine* database (** $P < 0.001$, $n = 59, 34$). **(d)** High PTPN11 expression levels are strongly correlated with shortened prostate tumor patient survival. Data were analyzed based on Grasso cancer prostate cancer gene expression study⁴⁴ in the *Oncomine* database ($P = 0.0176$, $n = 21$ in the PTPN11 high group, $n = 9$ in the PTPN11 low group). **(e)** Elevated protein levels of Shp2 are detected in 8 out of 14 fresh tumor samples compared with paired normal tissues. In the rest six pairs of samples, equivalent Shp2 protein levels between tumors and normal tissues are observed (N, normal tissue; T, tumor). **(f)** Immunohistochemical staining of prostate cancer and matched adjacent normal tissue with Shp2 antibody. Increased staining intensity is detected in 26 out of 43 tumors. Representative patient sample of Gleason score 7 was shown (scale bars = 60 μm).

LnCap cells, as evidenced by Boyden chamber assays (Figures 4b and c and Supplementary Figure S2D). In addition, expression of KD-Shp2 resulted in inhibited migration of DU145 cells (Figure 4d). We further applied a real-time microscopic imaging of LnCap cells to monitor the impact of Shp2 on the behavior of cells. As shown in the Supplementary Videos 1–3 and Supplementary Figure S3A, overexpression of WT-Shp2 or DA-Shp2 led to increased cell motility of LnCap cells. Moreover,

by using the Xcelligence real-time cell migration monitoring system (Roche, San Diego, CA, USA), we clearly showed that WT-Shp2 or DA-Shp2 overexpression resulted in enhanced migration of prostate cancer cells shortly after the seeding of cells (Supplementary Figure S3B), suggesting an essential role of Shp2 in controlling prostate cancer cell motility. To further substantiate this notion, we took advantage of an *in vivo* metastasis assay in which metastatic PC3 cells stably expressing

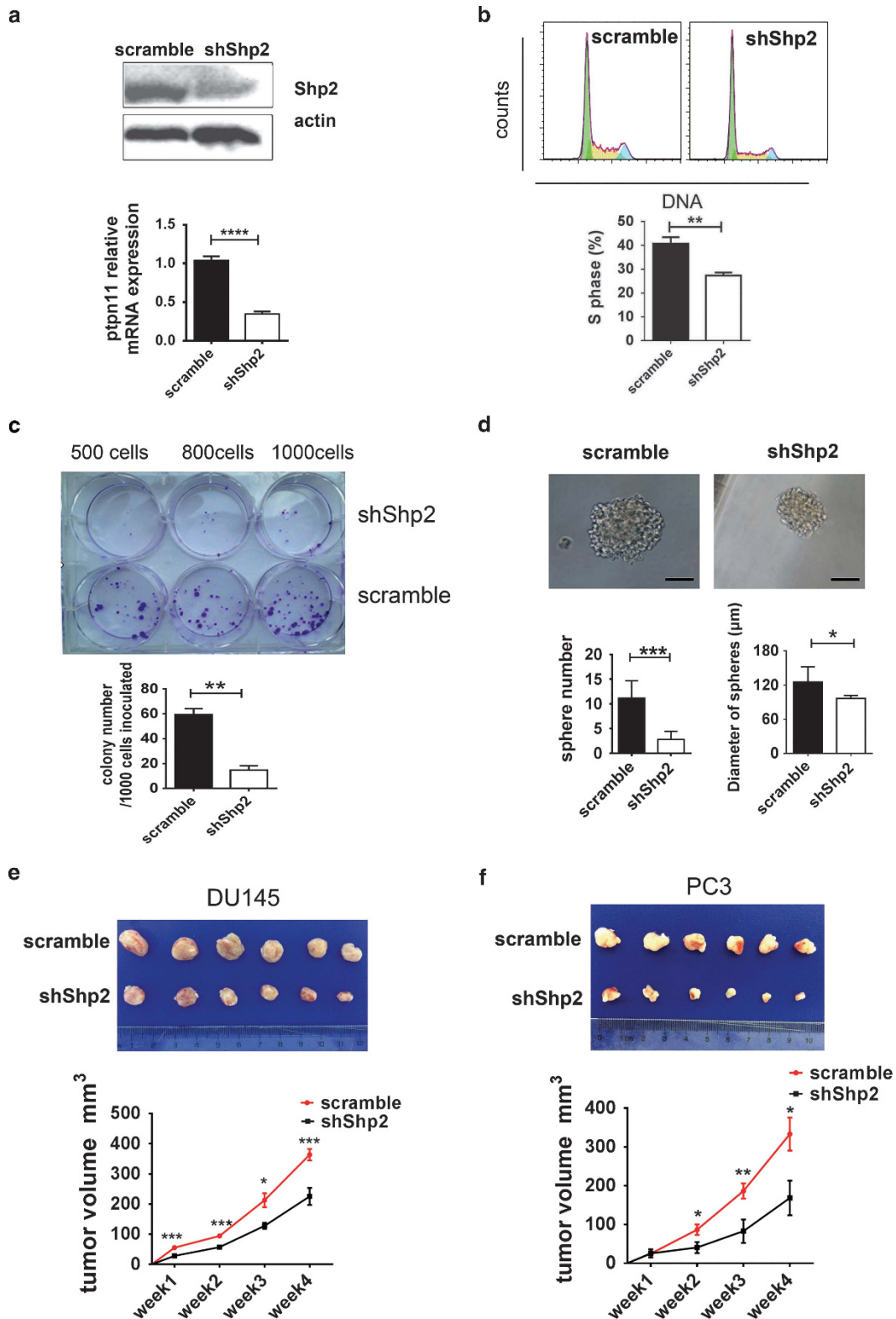


Figure 2. Shp2 knockdown inhibits prostate cell proliferation, colony and sphere formation *in vitro* and xenograft tumor growth *in vivo*. (a) Efficient knock down of Shp2 by shRNA lentivirus are confirmed by immunoblotting and q-RT-PCR. Experiments were repeated at least three times and representative images are shown. (b) Cell cycle analysis by propidium iodide (PI) staining shows that Shp2 knockdown slows down the cell cycle progression of DU145 cells ($n=3$). (c) Shp2 knockdown reduces the capability of clone formation of DU145 cells. (d) Knockdown of Shp2 inhibits DU145 cell sphere formation in the Matrigel (scale bars = 150 μm , $n=6$). (e) Shp2 gene silencing by shRNA leads to suppressed xenograft tumor growth of DU145 cells *in vivo* ($n=10$). (f) Shp2 knockdown slows down xenograft tumor growth of PC3 cells *in vivo* ($n=6$) (** $p < 0.001$, ** $p < 0.01$ data are shown as means \pm s.e.m.).

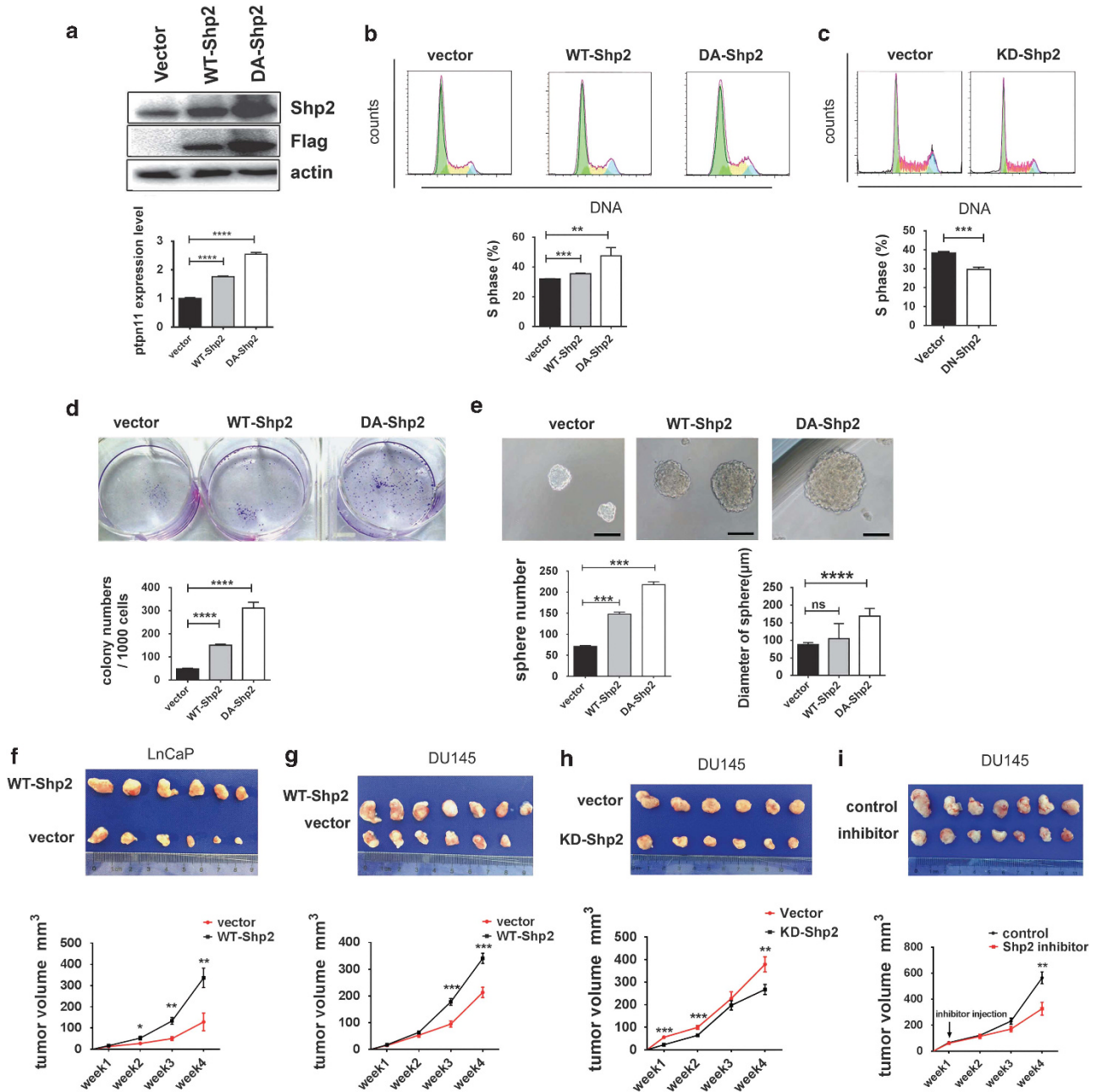


Figure 3. Shp2 overexpression promotes prostate cancer cell growth *in vitro* and *in vivo*. **(a)** Expression of flag-tagged WT and DA-Shp2 in retroviral-transfected LNCaP cells is verified by immunoblotting and q-RT-PCR. Experiments were repeated at least three times and representative images are shown. **(b)** Cell cycle analysis by propidium iodide (PI) staining indicates that overexpression of Shp2 accelerates LNCaP cell proliferation. Ectopic expression of DA-Shp2 further enhances the cell proliferation rate of LNCaP cells ($n = 3$). **(c)** Expression of KD-Shp2 leads to suppressed cell proliferation of DU145 cells. This effect is aggravated by DA-Shp2 expression ($n = 3$). **(d)** WT-Shp2 overexpression significantly promotes LNCaP cell colony formation. This effect is aggravated by DA-Shp2 expression ($n = 3$). **(e)** Sphere-forming assays show increased sphere numbers generated from LNCaP cells stably expressing WT-Shp2 and DA-Shp2 (scale bars = 150 μm , $n = 3$). **(f and g)** Shp2 overexpression promotes the xenograft tumor growth of LNCaP cells **(f)** and DU145 cells **(g)** ($n = 10$). **(h)** Expression of KD-Shp2 results in suppressed xenograft tumor growth of DU145 cells ($n = 10$). **(i)** *In vivo* treatment with Shp2 inhibitor IIB-08 represses the xenograft tumor growth of DU145 cells ($n = 10$). One week after the inoculation of DU145 cells, 100 mg/kg IIB-08 were injected intraperitoneally each day for 7 consecutive days into tumor bearing mice. Tumor size was monitored each week for 3 weeks after the treatment. Mice were killed at 4 weeks after inoculation for tumor collection and imaging.

luciferase were injected intracardially into nude mice, which were scanned by live animal bioluminescence imaging for metastasis detection 3 weeks after the inoculation. As shown in Figure 4e and Supplementary Figure S2E, PC3 cells transfected with scramble shRNA formed tumor foci in the femurs, lungs and heads of recipient mice, whereas Shp2 knockdown markedly suppressed the *in vivo* metastasis of PC3 cells. Additionally, ectopic expression

of KD-Shp2 in PC3 cells decreased the *in vivo* tumor cell metastasis (Figure 4f), suggesting that phosphatase activity of Shp2 was required for its metastasis-promoting effect.

Shp2 facilitates the EMT of prostate cancer cells

EMT, marked by loss of epithelial cell characteristics including cell-cell junctions, apical-basolateral cell polarity and gain of

mesenchymal cell features such as increased cell motility and expression of mesenchymal markers, has recently been reported to be an essential step for prostate cancer metastasis.⁵

Interestingly, when culturing the Shp2 knockdown DU145 cells, we found a more flat, polygonal epithelial-like shape compared with control DU145 cells, whereas LnCaP cells expressing WT-Shp2

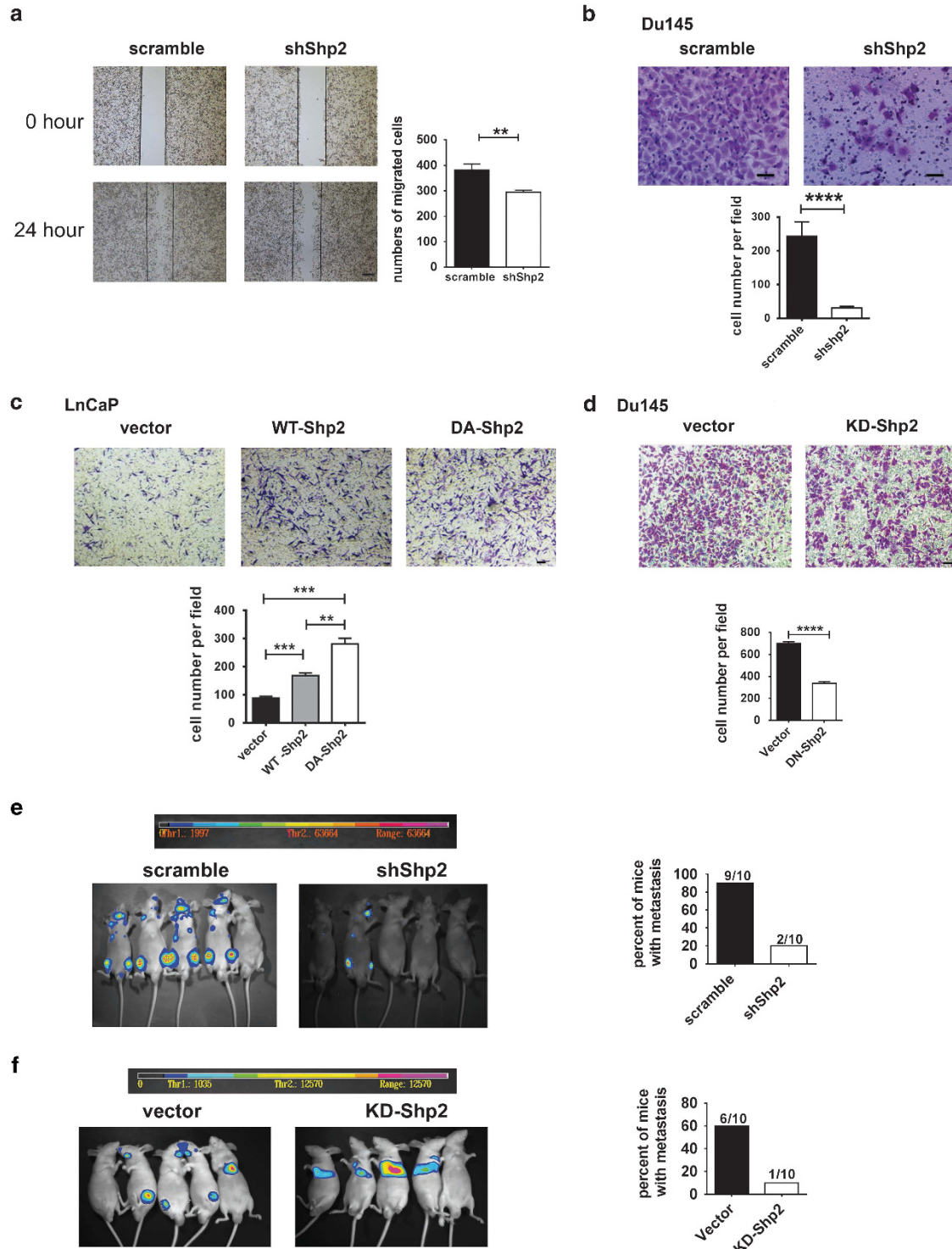


Figure 4. Shp2 promotes prostate cancer cell migration *in vitro* and metastasis *in vivo*. **(a)** Scratch assays shows inhibited cell motility of DU145 cells by Shp2 knockdown (scale bars = 50 μ m). **(b)** Shp2 gene silencing by shRNA suppresses the transwell migration of DU145 cells (scale bars = 50 μ m). **(c)** Expression of WT-Shp2 leads to increased transwell migration of LnCaP cells. Ectopic expression of DA-Shp2 caused an even higher migration rate of LnCaP cells (scale bars = 50 μ m). **(d)** DU145 cells stably expressing KD-Shp2 show significantly suppressed cell migration (scale bars = 50 μ m). **(e)** Shp2 knockdown inhibits prostate cancer cell metastasis *in vivo*. PC3-luciferase cells stably expressing Shp2-shRNA or scramble shRNA were injected, respectively, intracardially into the BALB/C nude mice. At 20 days postinjection, luminescent imaging was performed with a Xenogen IVIS Spectrum System ($n = 10$). **(f)** Expression of KD-Shp2 represses *in vivo* metastasis of PC3 prostate cancer cells ($n = 10$) (**** $P < 0.0001$, *** $P < 0.001$, ** $P < 0.01$, data are shown as means \pm s.e.m.).

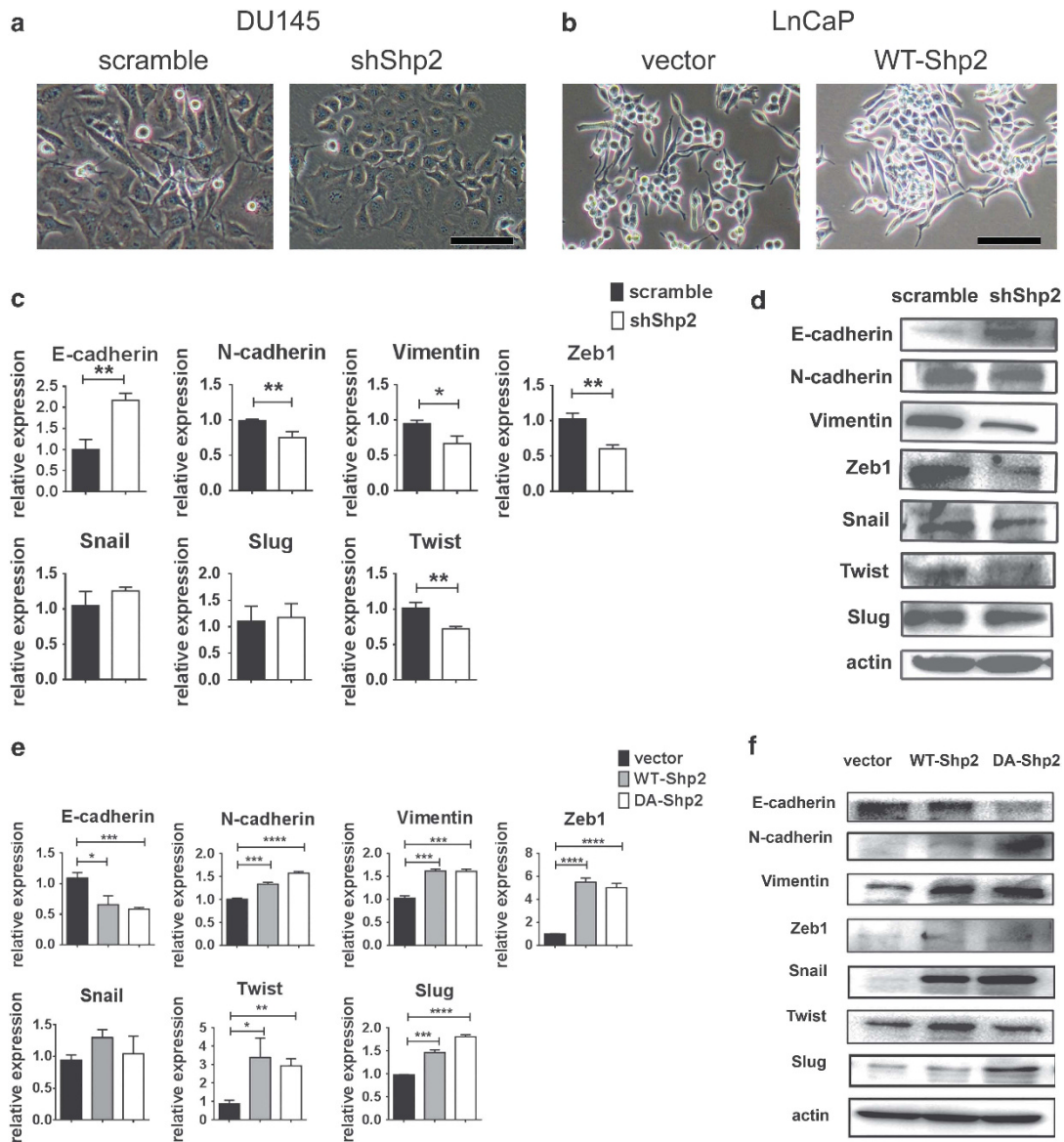


Figure 5. Shp2 promotes the EMT of prostate cancer cells. **(a)** Phase contrast images show that Shp2-knockdown DU145 cells display a more polygonal epithelial-like shape compared with control DU145 cells (scale bars = 100 μ m, multiple fields were examined under a microscope and representative pictures were shown). **(b)** Expression of WT-Shp2 induces a mesenchymal-like phenotype of LnCaP cells (scale bars = 100 μ m). **(c)** q-RT-PCR indicates upregulation of the epithelial-specific marker E-cadherin and downregulation of mesenchymal makers N-cadherin and vimentin, as well as the EMT-promoting transcriptional factor Zeb1 and Twist by Shp2 knockdown in DU145 cells. Experiments were repeated at least three times ($****P < 0.0001$, $***P < 0.001$, $**P < 0.01$, $*P < 0.05$, data are shown as means \pm s.e.m.). **(d)** Immunoblotting shows increased E-cadherin protein level and decreased protein levels of N-cadherin, vimentin, Zeb1, snail and Twist in DU145 cells transfected with Shp2-shRNA lentivirus. Experiments were repeated three times and representative pictures were shown. **(e)** Expression of WT-Shp2 or DA-Shp2 reduces the mRNA level of the epithelial-specific marker E-cadherin and increases the mRNA levels of mesenchymal makers N-cadherin and vimentin, as well as the EMT key transcriptional factors in LnCaP cells. Experiments were repeated at least three times ($****P < 0.0001$, $***P < 0.001$, $**P < 0.01$, $*P < 0.05$, data are shown as means \pm s.e.m.). **(f)** Immunoblotting shows suppressed E-cadherin protein level and elevated protein levels of N-cadherin, vimentin, Zeb1, snail and Twist in LnCaP cells expressing WT-Shp2. DA-Shp2 expression further decreases the expression of E-cadherin and enhances the expression of N-cadherin and slug. Experiments were repeated three times and representative pictures were shown.

adopted a more mesenchymal-like shape relative to the control cells (Figures 5a and b), suggesting that Shp2 is involved in the EMT of prostate cancer cells. In support of this, mRNA and protein levels of the epithelial cell-specific marker E-cadherin was significantly elevated in Shp2-knockdown DU145 cells (Figures 5c and d). Expression levels of the mesenchymal cell-specific markers N-cadherin and vimentin were notably suppressed upon Shp2 knockdown (Figures 5c and d). We then assessed expression

of the transcriptional factors essential to EMT regulation including Zeb1, Snail, Twist and Slug. As shown in Figures 5c and d, Zeb1 and Twist were downregulated in Shp2-knockdown DU145 cells. Consistently, expression of E-cadherin was significantly decreased, whereas N-cadherin and vimentin were upregulated in LnCaP cells infected with WT or DA-Shp2 retrovirus (Figures 5e and f). In addition, EMT-related transcriptional factors Zeb1, Snail and Slug were markedly induced by the ectopic expression of Shp2

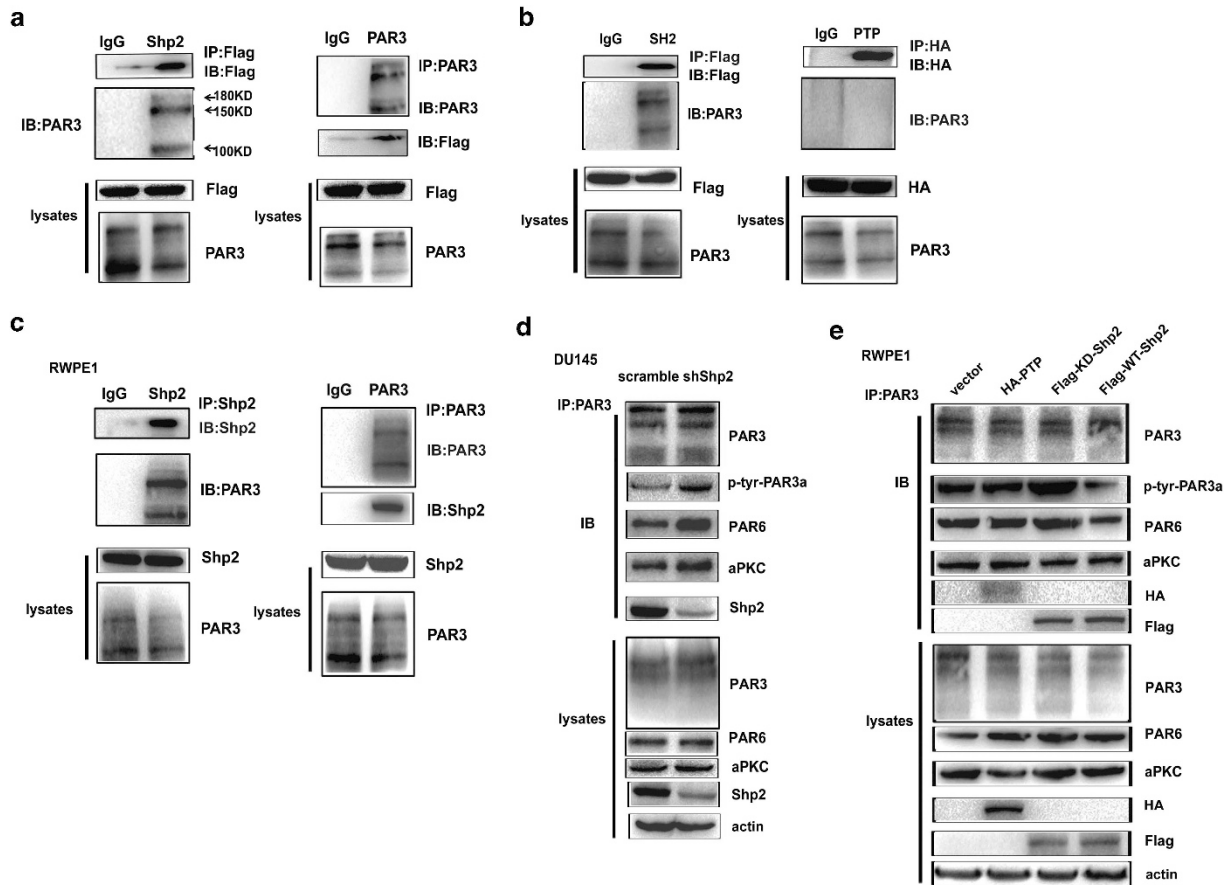


Figure 6. Shp2 binds to PAR3 via SH2 domain and attenuates the formation of PAR3/PAR6/aPKC polarity complex. **(a)** Shp2 co-immunoprecipitates with PAR3 in 293T cells transfected with PAR3 and flag-tagged Shp2. Cell lysates were immunoprecipitated with anti-Flag or anti-PAR3 antibodies respectively and then immunoblotted with indicated antibodies. **(b)** Plasmids expressing the flag-tagged two SH2 domains or the HA-tagged PTPase domain of Shp2 were transfected, respectively, to 293T cells. Co-immunoprecipitation experiments indicate an association between the SH2 domain of Shp2 and PAR3. **(c)** Endogenous Shp2 and PAR3 form protein complex in the prostate epithelial cell line RWPE1. RWPE1 cell lysates were immunoprecipitated with anti-Shp2 or anti-PAR3 antibodies, respectively, and then immunoblotted with indicated antibodies. **(d)** Shp2 knockdown leads to increased tyrosine phosphorylation of PAR3 and enhanced PAR3/PAR6/aPKC protein complex formation. Cell lysates from DU145 cells infected with shShp2 or scramble shRNA lentivirus were immunoprecipitated with anti-PAR3 antibody. Tyrosine phosphorylation of PAR3 was assessed by immunoblotting with anti-phospho-Tyr antibody. Co-precipitating PAR6 and aPKC and Shp2 were detected by immunoblotting using indicated antibodies. **(e)** Overexpression of WT-Shp2 results in suppression of PAR3 tyrosine phosphorylation and reduced PAR3/PAR6/aPKC protein interaction. Cell lysates from RWPE1 cells transfected with HA-tagged PTPase domain of Shp2, flag-tagged KD-Shp2 or flag-tagged WT-Shp2 or control retrovirus were immunoprecipitated with anti-PAR3 antibody, and then immunoblotted with anti-phospho-Tyr, anti-PAR6, anti-aPKC and anti-HA and anti-flag antibodies.

(Figures 5e and f). Taken together, these data indicate that Shp2 promotes EMT of prostate cancer cells, which might contribute to its stimulating role in tumor metastasis.

Shp2 interacts with PAR3, downregulates the tyrosine phosphorylation of PAR3 and attenuates the formation of PAR3/PAR6/aPKC polarity complex

Maintenance of apical–basal polarity and cell–cell junctions are essential for the normal structure and function of epithelial cells. Disruption of both biological features is frequently observed in premetastatic primary tumor sites and is believed to be an indispensable step for EMT.³ Previous studies suggested that Shp2 might indirectly contribute to the regulation of the PAR polarity protein complexes.^{12,26} We tackled this unsettled question by co-immunoprecipitation assays using antibodies against Shp2 or PAR proteins. As shown in Figure 6a, a physical interaction between Shp2 and PAR3 was detected in 293T cells. To further explore which domain of Shp2 is required for the Shp2/PAR3 interaction, we transfected 293 cells with two truncated forms of Shp2—that is, (1) the truncated Shp2 with two SH2 domains, and (2) the

truncated Shp2 with the PTPase domain, and then performed co-immunoprecipitation experiments. As shown in Figure 6b, the SH2 domains but not the PTPase domain of Shp2 associated with PAR3. Endogenous interactions between Shp2 and PAR3 were confirmed in the immortalized prostate epithelial cell line RWPE1 (Figure 6c). By forming the polarity complex with PAR6 and aPKC, PAR3 acts as an essential factor in the polarity machinery. Shp2 knockdown in DU145 cells resulted in increased amounts of the PAR6/PAR3/aPKC protein complex (Figure 6d). Consistently, we found that less PAR6 was co-immunoprecipitated with PAR3 from protein lysates of RWPE1 cells stably overexpressing Shp2 compared with that from lysates of the control group (Figure 6e). Furthermore, tyrosine phosphorylation level of PAR3 was increased in Shp2-knockdown DU145 cells and down-regulated in WT-Shp2-overexpressing RWPE1 cells compared with their respective controls (Figures 6d and e). KD-Shp2 overexpression led to enhanced tyrosine phosphorylation level of PAR3 (Figure 6e). Expression of the truncated Shp2 with PTPase domain, which was not able to interact with PAR3, did not affect the tyrosine phosphorylation level of PAR3 nor the PAR protein complex formation (Figure 6e). These data are consistent with

previous findings by Wang *et al.*¹¹ that tyrosine phosphorylation of PAR3 proteins by c-Yes and c-Src regulates epidermal growth factor receptor signaling-induced epithelial TJ formation.

It was reported that FAK was an important downstream effector of Shp2-mediated breast cancer cell migration.²³ To test if this mechanism was also involved in the regulation of prostate cancer cell migration, we first tested the phosphorylation level of FAK in Shp2-knockdown DU145 cells. As shown in Supplementary Figure S4A, the phospho-FAK was moderately upregulated upon Shp2 knockdown in non-stimulated prostate cancer cells, whereas the phospho-FAK level of scramble or shShp2-transfected prostate cells in response to epidermal growth factor stimulation was comparable. In addition, to further understand whether enhanced FAK activity was responsible for reduced cell migration of Shp2-knockdown cells, we applied a small-molecule FAK inhibitor PF-573228 in the cell migration assays. As shown in Supplementary Figure S4B, PF-573228 treatment did not rescue the suppressed cell migration by Shp2 knockdown. Collectively, these data suggested that FAK was not a major effector in the Shp2-mediated prostate cancer cell migration. This might be due to a tissue-specific context difference.

Shp2 overexpression disrupts the TJ and apical–basal polarity formation

To further understand the biological significance of Shp2-mediated signaling modulations on cell polarity, we performed immunofluorescent staining of E-cadherin, and TJ protein ZO-1 in polarized control MDCK (Madin-Darby canine kidney) cells or Shp2-overexpressing MDCK cells cultured on Transwell filters.

As shown in Figure 7a, confocal microscopy revealed that E-cadherin mainly distributed at the lateral membrane of vector-transfected MDCK cells. Overexpression of Shp2 led to decreased staining intensity and more apical distribution of E-cadherin in MDCK cells. ZO-1 was found exclusively to localize to the apical membrane of control MDCK cells. In contrast, a more diffuse distribution of ZO-1 was detected in the cytoplasm of Shp2-overexpressed MDCK cells, indicating a destruction of TJs (Figure 7b). To further explore the effect of Shp2 on polarized prostatic epithelial lumen formation, we performed *in vitro* epithelial lumen assay using MDCK cells or RWPE1 prostate epithelial cells. As shown in Figure 7c, control MDCK cells displayed apical staining of ZO-1 and produced single lumen epithelial ducts in the Matrigel, suggesting proper formation of apical–basal polarity. MDCK cells transfected with Shp2-expressing retrovirus failed to retain normal apical–basal polarity manifested by multiple positive ZO-1 staining regions and multilumen cyst formation in the Matrigel. Consistently, control RWPE1 cells formed epithelial ducts with a single hollow lumen (12 out of 20 spheroids examined), whereas RWPE1 cells overexpressing Shp2 hardly generated epithelial ducts with a single lumen (only 2 out of 20 spheroids examined showed an epithelial lumen structure), but rather formed cell aggregates when cultured in the Matrigel (Figure 7d).

DISCUSSION

Accumulating evidence has suggested that cell polarity is essential for the integrity of the epithelium.³² Disrupted cell polarity is demonstrated to affect symmetric/asymmetric cell division and

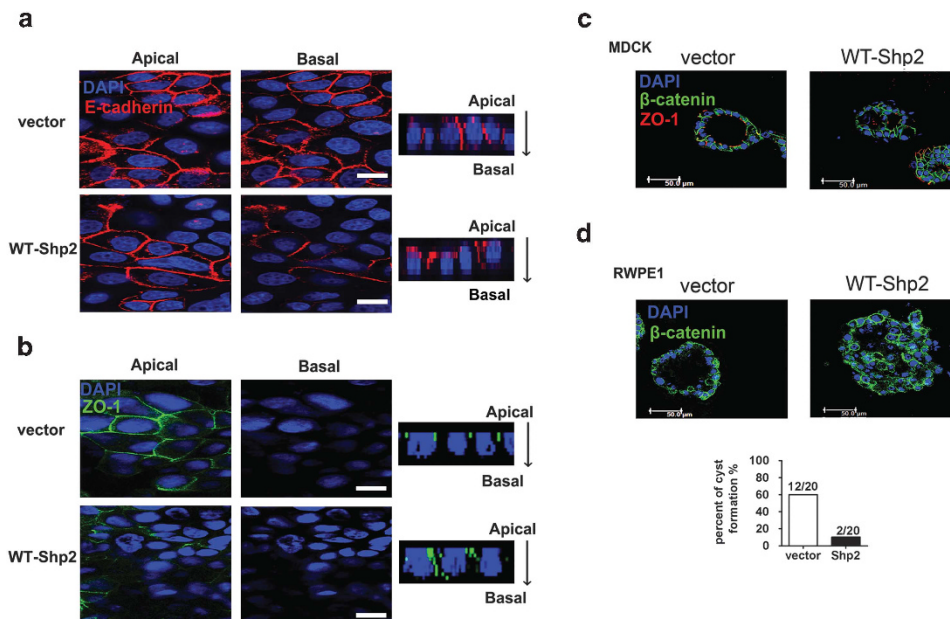


Figure 7. Shp2 overexpression disrupts the TJ and apical–basal polarity formation of epithelial cells. **(a)** Overexpression of Shp2 lead to more apical distribution of E-cadherin in MDCK cells in comparison with the normal lateral membrane localization of E-cadherin in control cells (scale bars = 10 μ m). **(b)** ZO-1 exclusively localizes to the apical membrane of polarized MDCK cells cultured on Transwell filters. Shp2 overexpression causes a more diffuse distribution of ZO-1 in the cytoplasm of MDCK cells, suggesting a disruption of TJs (scale bars = 10 μ m). **(c)** For the *in vitro* epithelial lumen assay, MDCK cells were cultured in the Matrigel for 10 days. Sphereroids were collected for immunofluorescent staining with anti- β -catenin (green) and anti-ZO-1 (red) antibodies for the detection of epithelial lumen structure. Control MDCK cells display apical staining of ZO-1 and form single lumen epithelial ducts, indicating proper formation of apical–basal polarity, whereas MDCK cells overexpressing Shp2 fail to generate normal apical–basal polarity manifested by multiple positive ZO-1 staining regions and multilumen cyst formation (scale bars = 50 μ m). **(d)** Shp2 overexpression disrupts the epithelial lumen formation of RWPE1 prostate epithelial cells. RWPE1 cells were cultured in the Matrigel for 2 weeks. Sphereroids were collected for immunofluorescent staining with anti- β -catenin (green) antibody. Note that control RWPE1 cells form epithelial ducts with a single hollow lumen, whereas RWPE1 cells transfected with Shp2 retrovirus can hardly generate epithelial ducts with single lumen, but rather form cell aggregates in the Matrigel (scale bars = 50 μ m).

tumorigenesis, and to be closely associated with EMT and tumor invasiveness.^{33,34} Our previous study in the Pten-knockout murine prostate tumor model indicates that disrupting the localization of the PAR3/aPKC complex at tight junctions in luminal cells leads to loss of cell polarity and dysregulated spindle orientation of dividing cells, resulting in accelerated prostatic hyperplasia.³⁵ However, how the cell polarity machinery is modulated by extracellular stimuli and intracellular signaling pathways are not fully understood. The present study provides a novel mechanism by which oncogenic signaling molecule regulates the PAR protein complex: Shp2 interacts with PAR3 via its SH2 domain, attenuates the phosphorylation of PAR3 and disrupts the formation of the PAR3/PAR6/aPKC polarity protein complex. As a consequence, cell polarity and cell–cell junctions are disrupted, and EMT is promoted. It was shown recently that PAR3 was an important factor in different tumor initiation and progression. Par3 knockout led to enhanced breast tumorigenesis and metastasis in mice, whereas Par3 exerted cell context-dependent oncogenic or tumor-suppressing roles in skin cancers.^{36,37} It is possible that PAR3 is also responsible for the positive effects of Shp2 on prostate cancer cell proliferation, sphere formation and *in vivo* tumor formation, besides its function in the regulation of cell polarity. On the other hand, considering the role of Shp2 in Ras and other signaling pathways, we do not exclude other signaling downstream effectors for the positive role of Shp2 in prostate tumors.

Interestingly, we find that Shp2 positively regulates EMT-related transcriptional factors. Ectopic expression of WT or DA-Shp2 leads to marked enhancement of mesenchymal phenotypes. It was recently shown that in breast cancer, Shp2 activates stemness-associated transcription factors, c-Myc and Zeb1, and contributes to the maintenance of breast cancer-initiating cells.²⁰ It remains to be further studied whether Shp2 and its modulated EMT transcriptional factors are required for the functions of prostate tumor stem cells.

Although androgen deprivation treatment, which currently serves as the first line of treatment for prostate cancer, is proven to be effective for the initial treatment, recurrence inevitably occurs in virtually every patient receiving androgen deprivation treatment.³⁸ Surgery and radiation therapy have also significantly improved patient survival, but effective treatment for advanced diseases, especially those with metastasis, is still lacking. Development of such cures requires further understanding of the underlying molecular mechanisms governing the prostatic tumor progression and metastasis. The present study demonstrates that upregulation of Shp2, a protein tyrosine phosphatase, is positively correlated with advanced prostate cancer stages. Functionally, Shp2 promotes prostate cancer cell proliferation, sphere formation, *in vivo* tumor formation and metastasis, suggesting a promoting role of Shp2 in the progression and metastasis of prostate cancer. Interestingly, although traditionally considered as a proto-oncogene in leukemias, Shp2 has recently been found to act as a tumor suppressor in liver cancer.^{16,17} A later study suggested that Shp2 dephosphorylates parafibromin and converts the latter from an antiproliferative factor to an activator of the oncogenic WNT- β -catenin signaling pathway.³⁹ Therefore, our findings together with other studies suggest a multifaceted role of Shp2 in tumorigenesis dependent on specific tumor context.

In conclusion, our study has revealed the biological and clinical significance of Shp2 in prostate cancer. Shp2 disrupts epithelial polarity, facilitates tumor cell motility and promotes metastasis by targeting the PAR3/PAR6/aPKC polarity complex. Pharmaceutical intervention of Shp2 alone or in combination with surgery or radiation therapy might provide a promising strategy to alleviate advanced tumor progression and metastasis.

MATERIALS AND METHODS

Cell culture

Du145 and PC3 prostate cancer cell lines were maintained in Dulbecco's modified Eagle's medium, whereas LnCaP cells were cultured in RPMI-1640 medium supplemented with 10% fetal bovine serum, 100 U/ml penicillin and 100 μ g/ml streptomycin. RWPE1 prostate epithelial cells were grown in keratinocyte serum-free medium (Gibco, Carlsbad, CA, USA; no. 17005-042). All the above cells were from American Type Culture Collection (Manassas, VA, USA), cultured at 37 °C incubators providing a humidified atmosphere with 5% CO₂ and tested for mycoplasma contamination.

Patient samples

Fresh prostate cancer patient samples were obtained from prostatectomy surgery at the Department of Urology from Ren Ji Hospital (Shanghai, China). All samples were collected, stored and used with informed consent of the patients. In addition, a total of 58-spot paraffin-embedded tissue array chip including 29 prostate cancer and paired normal tissues were purchased from Shanghai Outdo Biotech Ltd (Shanghai, China). The protocol for collection and usage of clinical samples was approved by Ren Ji Hospital Ethic Committee.

Plasmids and virus production and infection

shRNA against Shp2 and scramble shRNA were constructed into the lentiviral vector pLVTH as reported previously.⁴⁰ The shShp2 no. 2 plasmid MDH1-shSHP2-3-H2Kb2 was a gift from Dr Chang-Zheng Chen (Addgene, Cambridge, MA, USA; plasmid no. 17854). The cDNA of WT-Shp2, DA-Shp2 (Shp2 D61A mutant) and KD-Shp2 (Shp2 C459S mutant) with a C-terminal Flag-tag were cloned into the retroviral vector pLPCX. The expression plasmid for the Shp2 PTPase domain with HA tag was a kind gift from Dr Jianxiu Yu (Shanghai Jiao Tong University, Shanghai, China). The construct for the SH2 domains of Shp2 was generously provided by Dr Gen-Sheng Feng (University of California, San Diego, CA, USA). Lentivirus and retrovirus were produced as described previously.¹⁴ Prostate cancer cells were infected by lentivirus or retrovirus using spinoculation at 3000 r.p.m. for 1.5 h. To select cells expressing shRNA, green fluorescent protein-positive cells were sorted using BD Aria flow cytometry (BD, San Jose, CA, USA). For pLPCX retrovirus-infected cells, 5 μ g/ml puromycin was added to the culture medium for 2 weeks to generate stable expressing cell line.

Immunohistochemical and immunofluorescent staining

Immunohistochemical and immunofluorescent staining was performed as described before.⁴¹ Detailed descriptions of experimental procedures are available in Supplementary Materials and methods.

Quantitative RT-PCR

Total RNA was extracted using the Trizol reagent (Invitrogen, Carlsbad, CA, USA) according to the manufacturer's instruction. Detailed descriptions are provided in Supplementary Materials and methods.

Immunoprecipitation and immunoblotting

Immunoprecipitation and immunoblotting was performed as described before.⁴¹ Detailed descriptions are available in Supplementary Materials and methods.

Propidium iodide staining for cell cycle analysis

Cells were washed with phosphate-buffered saline (PBS) and then fixed with 70% methanol at –20 °C for at least 2 h. After fixation, cells were washed with PBS two times and incubated with 50 μ g/ml propidium iodide solution supplemented with 5 mg/ml DNase-free RNase in the dark at 37 °C for 30 min. The samples were analyzed immediately with a C6 flow cytometer (BD Biosciences, San Jose, CA, USA). Flow cytometry data were analyzed by the FlowJo software package (FLOWJO, LLC, Ashland, OR, USA).

Migration assay

In total, 3×10^4 DU145 cells or 5×10^4 LnCaP cells were plated on the top chambers of the Costar Transwell Migration Plates (8 μ m pore size; Corning, Lowell, MA, USA; no. 3422) with serum-free medium. To the bottom chamber, 500 μ l medium containing 20% fetal bovine serum was added. After 12 h of incubation, the inserts were washed with PBS buffer.

Migrated cells were fixed with 4% paraformaldehyde for 10 min, washed with PBS and stained with 0.1% crystal violet at room temperature for 5 min. For each insert, we took five random fields under a light microscope and counted manually. Experiments were performed in triplicate.

Colony-, sphere- and epithelial lumen-forming assays

Detailed descriptions of colony-, sphere- and epithelial lumen-forming assays are available in Supplementary Materials and methods.

In vivo xenograft tumor assay

A total of 5×10^6 LnCaP cells, 3×10^6 DU145 cells or 3×10^6 PC3 cells were suspended in 100 μ l PBS and mixed with 100 μ l matrigel (BD Biosciences). The mixtures were injected subcutaneously into 6-week male BALB/C nude mice (SLAC, Shanghai, China). The animals were randomized for treatment. Tumor volumes were measured every week from the second week after inoculation (tumor volume = tumor length \times tumor width²/2). At 4 weeks after inoculation, mice were killed and the tumors were collected and imaged. Tumor measurements were performed by blind investigator assessment. All experimental mice were housed in the pathogen-free animal facility of Ren Ji Hospital with controlled temperature and humidity. The animal experimental protocol was in compliance with Ren Ji Hospital animal care ethical regulations and approved by Ren Ji Hospital Animal Care Committee. The sample size was chosen to ensure statistical significance.

In vivo tumor metastasis experiment

PC3 cell line stably expressing luciferase was generously provided by Dr Jianhua Wang (Shanghai Jiao Tong University). A total of 5×10^6 PC3-luciferase cells were injected into the left ventricle of 6-week old male BALB/C nude mice. Twenty days after injection, mice were anesthetized with Avertin at a dosage of 250 mg/kg via intraperitoneal injection, then injected with 150 mg/kg D-luciferin (CellCyto, Shanghai, China) and imaged using the Xenogen IVIS Spectrum System (Perkin-Elmer, Waltham, MA, USA).

Statistical data analysis

Student's *t*-test was used for statistical analysis. Patient survival analysis was performed using log-rank (Mantel-Cox) test. A significant difference was defined when the *P*-value was < 0.05.

CONFLICT OF INTEREST

The authors declare no conflict of interest.

ACKNOWLEDGEMENTS

The study is supported by funds to W-Q Gao from the Chinese Ministry of Science and Technology (2012CB966800 and 2013CB945600), the National Natural Science Foundation of China (NSFC, 81130038 and 81372189), the Science and Technology Commission of Shanghai Municipality (Pujiang program), the Shanghai Health Bureau Key Discipline and Specialty Foundation, the Shanghai Education Committee Key Discipline and Specialty Foundation (J50208) and the KC Wong foundation, and by funds to HH Zhu from the NSFC (81270627), the Science and Technology Commission of Shanghai Municipality (Pujiang program 12PJ1406100) and the Shanghai Education Committee (Chenguang program 12CG16, 13YZ030 and young investigator program) and Shanghai Institutions of Higher Learning (The Program for Professor of Special Appointment (Young Eastern Scholar)).

REFERENCES

- Jemal A, Bray F, Center MM, Ferlay J, Ward E, Forman D. Global cancer statistics. *CA Cancer J Clin* 2011; **61**: 69–90.
- Shen MM, Abate-Shen C. Molecular genetics of prostate cancer: new prospects for old challenges. *Genes Dev* 2010; **24**: 1967–2000.
- Valastyan S, Weinberg RA. Tumor metastasis: molecular insights and evolving paradigms. *Cell* 2011; **147**: 275–292.
- Tam WL, Weinberg RA. The epigenetics of epithelial–mesenchymal plasticity in cancer. *Nat Med* 2013; **19**: 1438–1449.
- Li P, Yang R, Gao WQ. Contributions of epithelial–mesenchymal transition and cancer stem cells to the development of castration resistance of prostate cancer. *Mol cancer* 2014; **13**: 55.

- Etienne-Manneville S. Polarity proteins in migration and invasion. *Oncogene* 2008; **27**: 6970–6980.
- Goldstein B, Macara IG. The PAR proteins: fundamental players in animal cell polarization. *Dev Cell* 2007; **13**: 609–622.
- Macara IG. Parsing the polarity code. *Nat Rev Mol Cell Biol* 2004; **5**: 220–231.
- Suzuki A, Ohno S. The PAR–aPKC system: lessons in polarity. *J Cell Sci* 2006; **119**: 979–987.
- Aranda V, Haire T, Nolan ME, Calarco JP, Rosenberg AZ, Fawcett JP *et al*. Par6–aPKC uncouples ErbB2 induced disruption of polarized epithelial organization from proliferation control. *Nat Cell Biol* 2006; **8**: 1235–1245.
- Wang Y, Du D, Fang L, Yang G, Zhang C, Zeng R *et al*. Tyrosine phosphorylated Par3 regulates epithelial tight junction assembly promoted by EGFR signaling. *EMBO J* 2006; **25**: 5058–5070.
- Saadat I, Higashi H, Obuse C, Umeda M, Murata-Kamiya N, Saito Y *et al*. Helicobacter pylori CagA targets PAR1/MARK kinase to disrupt epithelial cell polarity. *Nature* 2007; **447**: 330–333.
- Zhu HH, Feng GS. The dynamic interplay between a PTK (Kit) and a PTP (Shp2) in hematopoietic stem and progenitor cells. *Cell Cycle* 2011; **10**: 2241–2242.
- Zhu HH, Ji K, Alderson N, He Z, Li S, Liu W *et al*. Kit–Shp2–Kit signaling acts to maintain a functional hematopoietic stem and progenitor cell pool. *Blood* 2011; **117**: 5350–5361.
- Tartaglia M, Gelb BD. Noonan syndrome and related disorders: genetics and pathogenesis. *Annu Rev Genomics Hum Genet* 2005; **6**: 45–68.
- Chan RJ, Feng GS. PTPN11 is the first identified proto-oncogene that encodes a tyrosine phosphatase. *Blood* 2007; **109**: 862–867.
- Bard-Chapeau EA, Li S, Ding J, Zhang SS, Zhu HH, Princen F *et al*. Ptpn11/Shp2 acts as a tumor suppressor in hepatocellular carcinogenesis. *Cancer Cell* 2011; **19**: 629–639.
- Sausgruber N, Coissieux MM, Britschgi A, Wyckoff J, Aceto N, Leroy C *et al*. Tyrosine phosphatase SHP2 increases cell motility in triple-negative breast cancer through the activation of SRC-family kinases. *Oncogene* 2014; **34**: 2272–2278.
- Schneeberger VE, Luetkeke N, Ren Y, Berns H, Chen L, Foroutan P *et al*. SHP2E76K mutant promotes lung tumorigenesis in transgenic mice. *Carcinogenesis* 2014; **35**: 1717–1725.
- Aceto N, Sausgruber N, Brinkhaus H, Gaidatzis D, Martiny-Baron G, Mazarrol G *et al*. Tyrosine phosphatase SHP2 promotes breast cancer progression and maintains tumor-initiating cells via activation of key transcription factors and a positive feedback signaling loop. *Nat Med* 2012; **18**: 529–537.
- Bentires-Alj M, Paez JG, David FS, Keilhack H, Halmos B, Naoki K *et al*. Activating mutations of the Noonan syndrome-associated SHP2/PTPN11 gene in human solid tumors and adult acute myelogenous leukemia. *Cancer Res* 2004; **64**: 8816–8820.
- Wang FM, Liu HQ, Liu SR, Tang SP, Yang L, Feng GS. SHP-2 promoting migration and metastasis of MCF-7 with loss of E-cadherin, dephosphorylation of FAK and secretion of MMP-9 induced by IL-1beta *in vivo* and *in vitro*. *Breast Cancer Res Treat* 2005; **89**: 5–14.
- Hartman ZR, Schaller MD, Agazie YM. The tyrosine phosphatase SHP2 regulates focal adhesion kinase to promote EGF-induced lamellipodia persistence and cell migration. *Mol Cancer Res* 2013; **11**: 651–664.
- Yang X, Dutta U, Shaw LM. SHP2 mediates the localized activation of Fyn downstream of the alpha6beta4 integrin to promote carcinoma invasion. *Mol Cell Biol* 2010; **30**: 5306–5317.
- Zhou XD, Agazie YM. Inhibition of SHP2 leads to mesenchymal to epithelial transition in breast cancer cells. *Cell Death Differ* 2008; **15**: 988–996.
- Yang Z, Xue B, Urimitsu M, Ikura M, Muthuswamy SK, Neel BG. The signaling adaptor GAB1 regulates cell polarity by acting as a PAR protein scaffold. *Mol Cell* 2012; **47**: 469–483.
- Bard-Chapeau EA, Yuan J, Droin N, Long S, Zhang EE, Nguyen TV *et al*. Concerted functions of Gab1 and Shp2 in liver regeneration and hepatoprotection. *Mol Cell Biol* 2006; **26**: 4664–4674.
- Wohrle FU, Daly RJ, Brummer T. Function, regulation and pathological roles of the Gab/DOS docking proteins. *Cell Commun Signal* 2009; **7**: 22.
- Feng GS, Hui CC, Pawson T. SH2-containing phosphotyrosine phosphatase as a target of protein-tyrosine kinases. *Science* 1993; **259**: 1607–1611.
- Mali RS, Ma P, Zeng LF, Martin H, Ramdas B, He Y *et al*. Role of SHP2 phosphatase in KIT-induced transformation: identification of SHP2 as a druggable target in diseases involving oncogenic KIT. *Blood* 2012; **120**: 2669–2678.
- Kodama A, Matozaki T, Fukuhara A, Kikyo M, Ichihashi M, Takai Y. Involvement of an SHP-2-Rho small G protein pathway in hepatocyte growth factor/scatter factor-induced cell scattering. *Mol Biol Cell* 2000; **11**: 2565–2575.
- Martin-Belmonte F, Perez-Moreno M. Epithelial cell polarity, stem cells and cancer. *Nat Rev Cancer* 2012; **12**: 23–38.
- Knoblich JA. Mechanisms of asymmetric stem cell division. *Cell* 2008; **132**: 583–597.

- 34 Huang L, Muthuswamy SK. Polarity protein alterations in carcinoma: a focus on emerging roles for polarity regulators. *Curr Opin Genet Dev* 2010; **20**: 41–50.
- 35 Wang J, Zhu HH, Chu M, Liu Y, Zhang C, Liu G *et al*. Symmetrical and asymmetrical division analysis provides evidence for a hierarchy of prostate epithelial cell lineages. *Nat Commun* 2014; **5**: 4758.
- 36 McCaffrey LM, Montalbano J, Mihai C, Macara IG. Loss of the Par3 polarity protein promotes breast tumorigenesis and metastasis. *Cancer Cell* 2012; **22**: 601–614.
- 37 Iden S, van Riel WE, Schafer R, Song JY, Hirose T, Ohno S *et al*. Tumor type-dependent function of the par3 polarity protein in skin tumorigenesis. *Cancer Cell* 2012; **22**: 389–403.
- 38 Karantanos T, Corn PG, Thompson TC. Prostate cancer progression after androgen deprivation therapy: mechanisms of castrate resistance and novel therapeutic approaches. *Oncogene* 2013; **32**: 5501–5511.
- 39 Takahashi A, Tsutsumi R, Kikuchi I, Obuse C, Saito Y, Seidi A *et al*. SHP2 tyrosine phosphatase converts parafibromin/Cdc73 from a tumor suppressor to an oncogenic driver. *Mol Cell* 2011; **43**: 45–56.
- 40 Lu Y, Xiong Y, Huo Y, Han J, Yang X, Zhang R *et al*. Grb-2-associated binder 1 (Gab1) regulates postnatal ischemic and VEGF-induced angiogenesis through the protein kinase A-endothelial NOS pathway. *Proc Natl Acad Sci USA* 2011; **108**: 2957–2962.
- 41 Zhou Z, Ji Z, Wang Y, Li J, Cao H, Zhu HH *et al*. TRIM59 is up-regulated in gastric tumors, promoting ubiquitination and degradation of p53. *Gastroenterology* 2014; **147**: 1043–1054.
- 42 Liu P, Ramachandran S, Ali Seyed M, Scharer CD, Laycock N, Dalton WB *et al*. Sex-determining region Y box 4 is a transforming oncogene in human prostate cancer cells. *Cancer Res* 2006; **66**: 4011–4019.
- 43 Yu YP, Landsittel D, Jing L, Nelson J, Ren B, Liu L *et al*. Gene expression alterations in prostate cancer predicting tumor aggression and preceding development of malignancy. *J Clin Oncol* 2004; **22**: 2790–2799.
- 44 Grasso CS, Wu YM, Robinson DR, Cao X, Dhanasekaran SM, Khan AP *et al*. The mutational landscape of lethal castration-resistant prostate cancer. *Nature* 2012; **487**: 239–243.

Supplementary Information accompanies this paper on the Oncogene website (<http://www.nature.com/onc>)